Improved Control Strategy of Grid-Forming Inverters for Fault-Ride Through in a Microgrid System

Preprint

Jing Wang

National Renewable Energy Laboratory

To be presented at the IEEE Energy Conversion Congress and Expedition (ECCE)
Detroit, Michigan
October 9–13, 2022

NREL is a national laboratory of the U.S. Department of Energy
Office of Energy Efficiency & Renewable Energy
Operated by the Alliance for Sustainable Energy, LLC

This report is available at no cost from the National Renewable Energy Laboratory (NREL) at www.nrel.gov/publications.

Contract No. DE-AC36-08GO28308

Conference Paper
NREL/CP-5D00-82049
August 2022

Improved Control Strategy of Grid-Forming Inverters for Fault-Ride Through in A Microgrid System

Preprint

Jing Wang

National Renewable Energy Laboratory

Suggested Citation
Wang, Jing. 2022. *Improved Control Strategy of Grid-Forming Inverters for Fault-Ride Through in a Microgrid System: Preprint*. Golden, CO: National Renewable Energy Laboratory. NREL/CP-5D00-82049. https://www.nrel.gov/docs/fy22osti/82049.pdf.

NREL is a national laboratory of the U.S. Department of Energy
Office of Energy Efficiency & Renewable Energy
Operated by the Alliance for Sustainable Energy, LLC

This report is available at no cost from the National Renewable Energy Laboratory (NREL) at www.nrel.gov/publications.

Contract No. DE-AC36-08GO28308

Conference Paper
NREL/CP-5D00-82049
August 2022

National Renewable Energy Laboratory
15013 Denver West Parkway
Golden, CO 80401
303-275-3000 • www.nrel.gov

NOTICE

This work was authored by the National Renewable Energy Laboratory, operated by Alliance for Sustainable Energy, LLC, for the U.S. Department of Energy (DOE) under Contract No. DE-AC36-08GO28308. This work was supported by the Laboratory Directed Research and Development (LDRD) Program at NREL. The views expressed herein do not necessarily represent the views of the DOE or the U.S. Government.

Improved Control Strategy of Grid-Forming Inverters for Fault Ride-Through in a Microgrid System

Jing Wang
National Renewable Energy Laboratory, Golden, CO 80401 USA
jing.wang@nrel.gov

***Abstract*— This paper develops an improved control strategy of grid-forming (GFM) inverters with fault ride-through (FRT) capabilities to guarantee the stable operation of microgrids under fault conditions, especially islanded microgrids and asymmetrical faults. The proposed control strategy includes the dual control of positive-sequence and negative-sequence control as well as the adaptive virtual impedance (VI) control. Unlike existing works, the proposed strategy applies the VI control for only the d component of the positive-sequence control and leaves the *q* component of the positive-sequence control and the *dq* component of the negative-sequence control as zero, thus achieving improved stability and balanced three-phase voltages under asymmetrical faults. The adaptive feature of the VI control guarantees the stability of the GFM inverter under severe faults, which could cause the saturation of the inner current loop, and the instability if the VI is not adaptive. Simulation results of various unbalanced faults with high and low fault impedances show that the proposed control strategy improves the stability of the GFM inverter and achieves stable and balanced output voltages in islanded microgrids. And the algorithm also improves the stability of GFM inverters under balanced faults with high and low fault impedances.**

Keywords—Asymmetrical faults, adaptive virtual impedance control, fault ride-through, grid-forming inverter.

I. Introduction

Grid-forming (GFM) inverters are going to become important grid assets for future electric grids, especially for microgrids, because of their grid-forming capability and superior stability compared to traditional grid-following (GFL) inverters [1]. Most existing control strategies of GFM inverters focus on normal operation to achieve voltage and frequency stability in microgrids under different operation modes; however, the operation of GFM inverters under fault conditions needs more attention because GFM inverters without fault ride-through (FRT) control can be subject to instability under some fault conditions, especially in islanded microgrids with all inverter-based resources. Several research works propose FRT strategies, such as [2]–[4], to limit inverter currents and prevent instability; however, those works consider only symmetrical faults or switch from voltage control to current control, and they do not provide grid-forming capabilities with needed negative-sequence current at the occurrence of asymmetrical faults (which are more common in reality). Several works study voltage control under asymmetrical faults, such as dual control, current and voltage limiting, and virtual impedance (VI) control [5]–[7].

Those methods consider either only dual control or impedance control, which might not achieve the best stability under asymmetrical faults. Further, there is no unified control for GFM inverters with the GFM capabilities in both grid-connected and islanded mode; therefore, this paper aims to develop an improved control strategy of GFM inverters with FRT capabilities to provide negative-sequence current and guarantee the stable operation of islanded microgrids under fault conditions. The desired FRT capabilities of a GFM inverter include: 1) maintain the stability and output voltage balance to stabilize the islanded microgrid system; 2) limit the fault current and avoid hardware damage to the inverter; and 3) achieve IEEE 1547-2018 compliance in grid-connected mode.

The main contributions of this paper can be summarized as follows: the paper 1) designs different control strategies of the FRT capabilities/response of a GFM inverter in grid-connected and islanded mode; 2) presents the fundamental reasons why the dual control structure is needed for GFM inverters to achieve stability and balanced voltage under asymmetrical faults to have FRT capability; 3) proposes an innovative adaptive VI control with the dual control structure and demonstrates its efficacy of compensating the unbalanced voltage caused by asymmetrical faults; and 4) tests the proposed adaptive VI control under both symmetrical and asymmetrical faults with high and low fault impedances, and further demonstrates the efficacy of the dual control structure and adaptive VI control for FRT capability.

The remainder of this manuscript is organized as follows: Section II describes the generic control structure of GFM inverters and identifies the different FRT control strategies of a GFM inverter in grid-connected and islanded mode. Section III investigates a GFM inverter's behavior under fault conditions and especially focuses on the asymmetrical faults. Section IV proposes the improved control strategy of GFM inverters with dual control structure and adaptive impedance control. And Section V presents the simulation of a microgrid with one GFM inverter under asymmetrical and symmetrical faults in islanded mode, and the 1547-2018 compliance testing in grid-connected mode is also tested and validated.

II. Control Algorithm of GFM Inverters

A typical double-loop controlled GFM inverter in a synchronous reference frame is presented in Figure 1. The same voltage and current controller are used for the inverter level control, no phase-locked loop (PLL) is needed, and the power level control is adjusted according to the status of two circuit breakers, S_0 and S_1. Only if S_0 and S_1 are "closed," which indicates a grid-connected operation condition, can P^* and Q^* (the active and reactive power references) and the integrator be enabled to allow the GFM inverter to generate the commanded power; otherwise, the GFM inverter only works in droop control mode, without P^* and Q^* and the integrator for power sharing in islanded mode. Note that this GFM inverter needs a sync check unit at S_1 to connect to the main grid during startup because it does not use the grid voltage for synchronization [8].

Based on the IEEE Std 1547-2018, the grid-connected inverter needs to follow the FRT and trip settings. That means the GFM inverters in grid-connected mode must follow the FRT and trip settings as well. In this regard, there is no need to design the improved control for GFM inverter in grid-connected mode. However, the GFM must have FRT capabilities to maintain the system in islanded mode because if the GFM inverters in islanded microgrid trip off due to the FRT and trip settings set as in grid-connected mode, there is no GFM sources in the islanded system for a 100% renewable microgrid. Thus, the strategy of controlling a GFM inverter is to separate the requirements of FRT capabilities in grid-connected and islanded mode: 1) IEEE 1547-2018 compliant in grid-connected mode and 2) integrating FRT controls in the existing control structure in islanded mode. Fig. 1 (b) illustrates this control strategy with grid-connected mode marked in red and islanded mode marked in blue.

For grid-connected mode, the grid side voltage V_{gabc} is used to extract the voltage RMS and frequency for IEEE 1547-2018 evaluation. If the IBR is GFL inverter, the implementation of DER response to abnormal voltage and frequency is straightforward: 1) for frequency, the augmented active power reference is calculated based on the frequency and the corresponding droop, and the inverter is required to trip after the threshold time; and 2) for voltage, the inverter can generate the active and reactive power as pre-fault for certain time with moderate fault voltage, and it has to go to momentary cessation (first five cycles with pre-fault power and zero power afterwards) or cease to energize (zero power) with extreme fault voltages. Essentially, the GFL DER response to be IEEE 1547 compliant is the adjustment of the active and reactive power output based on the required power response, and tripping of the circuit breaker after the threshold time. This is achievable as the GFL inverter still synchronizes with the grid voltage during fault, and it can generate the accurate power as requested.

For the GFM inverter, it can be controlled to provide required DER response to abnormal voltages because the adjustment of power output is either pre-fault values or zero. In order to make the GFM inverter generate zero power while still connected, e.g., momentary cessation/cease to energize, the voltage references (V_{od}^*, V_{oq}^*) and current references (i_{id}^*, i_{iq}^*) need to be zero instead of making the power references (P^*, Q^*) zero as shown in Fig. 1 (b). As for the GFM inverter response to abnormal frequencies, it depends on if the GFM inverter still can generate the required active power based on the droop characteristics. During the faults, the GFM inverter self-generated phase angle may not synchronize with the grid voltage anymore and the GFM inverter may not be able to respond accurately. This is out of the scope of this paper, and we will investigate it in future work.

For the islanded mode, there is no need for the GFM inverter to provide the DER response to abnormal voltage and frequency. Instead, integrating FRT controls in the existing control structure is recommended, and this will be the main focus of the rest of the paper. We will start from investigating the behavior of a GFM inverter under asymmetrical faults during islanded mode, then design FRT control correspondingly.

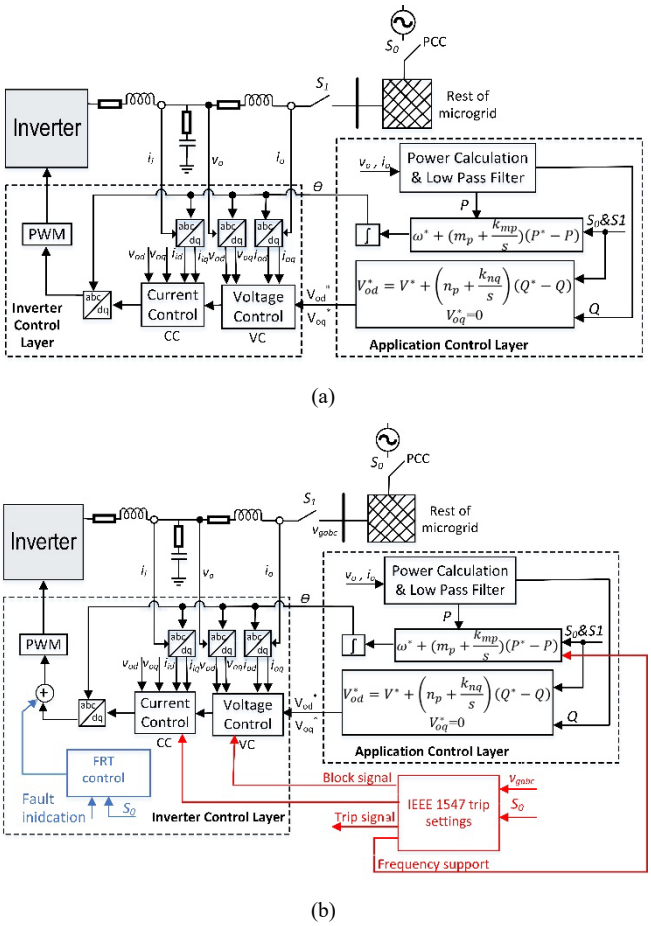

Fig. 1. Unified control structure of a GFM inverter working in grid-connected and islanded mode: (a) normal operation; and (b) fault responses.

III. Investigation of a GFM Inverter's Behavior Under Fault Conditions

A. Thevenin Equivalent Cicuirt of Asymmetrical Faults

To understand the behavior of a GFM inverter under unsymmetrical faults, it is necessary to study the sequence circuits to find the fault voltage and fault current during those faults. There are three types of unsymmetrical faults: single-line-to-ground (1LG), line-to-line (LL), and double-line-to-ground (2LG) faults. The Thevenin equivalent circuits of the system under those faults are shown in Fig. 2. It is not hard to understand that the 2LG fault has only negative-sequence current, and the other two have both negative- and zero-sequence currents.

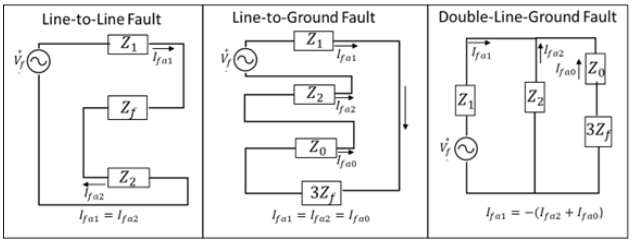

Fig. 2. Thevenin equivalent circuits under unbalanced faults [9].

B. Inverter Behavior with Asymmetrical Faults

For a system without unsymmetrical faults or unbalanced loads, the double-loop controlled GFM inverter shown in Fig. 1 should function well because there is only a positive-

sequence component in the system; however, when there are unsymmetrical faults or unbalanced loads, the voltage and current controller will be impacted because the *dq* components will no longer be in a DC quantity, as shown in Table 1; instead, the *dq* components will include both positive-sequence and negative-sequence elements.

Table 1 Sequence components in *dq* frame [10].

Element	Positive Sequence	Negative Sequence	Zero Sequence
V_d	V_1	$V_2\cos(2\omega t)$	0
V_q	0	$V_2\sin(2\omega t)$	0
V_o	0	0	$V_0\sin(\omega t)$

As we know, a PI control is a first-order controller, and a signal with sin and cos elements is second order; a first-order controller cannot track the second-order signal. Thus, the voltage and current controllers will have tracking errors, and the worst-case scenario is that the inner current loop is saturated, and the inverter output voltage and current are distorted or unstable. Fig. 3 shows the example results of a GFM inverter under a 2LG fault with different fault impedances (600 Ω for the top and 50 Ω for the bottom) in an islanded microgrid. Note that the inverter rated LL voltage is 480 V, and a Yg-Δ transformer is used to connect the GFM inverter with the rest of the grid (12 kV). Fig. 3 shows that the system is stable with a less severe fault, whereas it is unstable with a severe fault. When the GFM inverter is stable, the *dq* components exhibit ripples, which are the negative-sequence components caused by the 2LG fault. The voltage controller cannot track the reference. When the GFM inverter is unstable, the *dq* components exhibit strange waveforms, and the output voltage and current of the GFM inverters are highly distorted and abnormal.

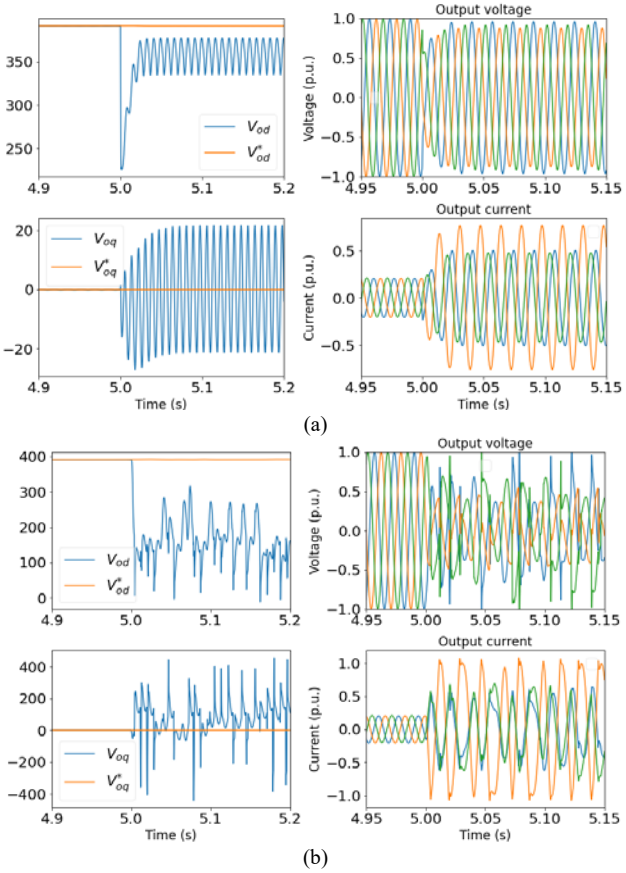

(a)

(b)

Fig. 3. A GFM inverter's behavior under a 2LG fault with different fault grid impedances: (a) 600 Ω and (b) 50 Ω fault impedance.

IV. Improved Control Strategy of GFM Inverters for FRT Capabilities

As noted in Section III, negative-sequence components exist in the *dq* components of the voltage and current controllers. To maintain the stability and balance of the GFM inverter under unsymmetrical faults, it is necessary to design the negative-sequence controller to compensate for the unbalance; therefore, this section proposes the improved control strategy of GFM inverters with FRT capabilities by designing a negative-sequence control in addition to the existing positive-sequence controller.

A. Dual Control Structure of the Improved Control Strategy of GFM Inverters

The improved control strategy of GFM inverters with both positive- and negative-sequence control is presented in Fig. 4 (a). A double-decoupled synchronous reference frame (SRF)-PLL is used to extract the positive- and negative-sequence components. The schematic diagram is presented in Fig. 4 (b). The capacitor voltage, v_o, is used to extract the phase angle θ', which is used for the SRF-PLL of the inverter current (i_i) and the grid-side current (i_o). After extracting the positive- and negative-sequences for v_o, i_i, and i_o, their positive-sequence components enter the voltage and current control; the process is the same for the negative sequence. For the negative-sequence control, the goal is to cancel them out; therefore, the voltage references, v_{od}^* and v_{oq}^*, are both zero. Note that the negative-sequence control is superimposed onto the positive-sequence control, and its effect is already negative by comparing it to the "0" reference; thus, the sign should be "negative" to achieve the cancelled effect. The ratio of the negative to positive component of the grid-side current (i_o), is used to select the negative-sequence control because there are not always faults/high-level unbalance in the system. For the power control level, the only difference is that the active and reactive power are calculated based on the positive-sequence component to have a smooth frequency and voltage reference.

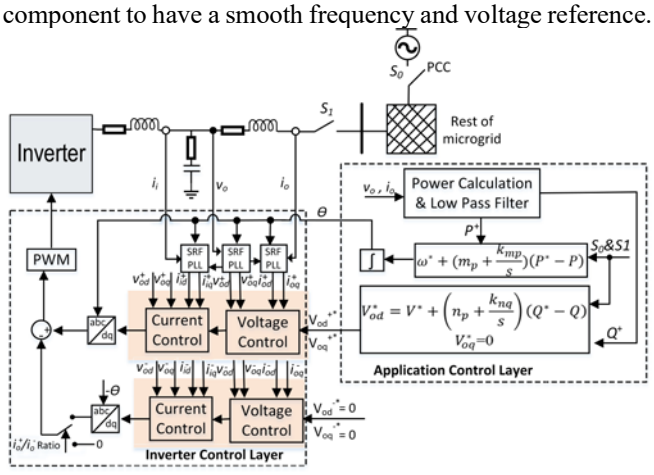

(a)

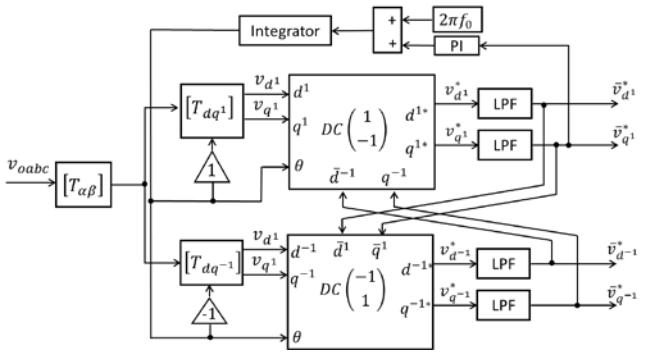

(b)

Fig. 4. (a) An improved control diagram with the negative-sequence controller for the GFM inverter and (b) a control diagram of the double-decoupled SRF-PLL for extracting the positive- and negative-sequence components [10].

B. *Virtual Impedance Control*

The VI control is added to the voltage control loop to soften the voltage reference because the fault generates a large fault current and causes the voltage to drop, and it is hard for the GFM inverter to achieve the target voltage reference. Otherwise, large amounts of fault current will be generated to pull the inverter's voltage down and saturate the inner current loop, and then the inverter becomes unstable. The VI control is added to the voltage control loop through an algebraic manipulation of the *dq* voltage reference signals, which is shown as follows:

$$V_{od}^{+*} = V_{od}^{+*} - \left(Ri_{od}^{+} - Xi_{oq}^{+}\right) \quad (1)$$

with R and X being the virtual resistance and reactance, respectively. Unlike the existing methods, only the *d*-axis voltage reference is modified by the VI control because the *q*-axis is usually zero even with faults, and there is no large voltage drop. Also, we still target achieving balanced voltage at the capacitor of the GFM inverter; therefore, the negative-sequence voltage references (V_{od}^{-*}, V_{oq}^{-*}) are still zero. This modification improves the stability of the GFM inverter under fault conditions, and the voltage of the GFM inverter is compensated to be balanced. Even though this is a small change to the existing methods, its improvement to the stability of the GFM inverter under fault conditions is significant.

C. *Adaptive Virtual Impedance Control*

Because different type of faults imposes different challenges/impacts to the GFM inverter controller, the fixed virtual impedance may only work effectively under some fault conditions. More simulations are performed with the 2LG, 1LG, LL and 3LG faults to further validate the negative-sequence control with the VI strategy. We realize that the 1LG faults are more severe and can significantly reduce the inverter voltage; thus, there is a need to retune the virtual impedance to improve the tracking performance and stability of the GFM inverters.

The R and X values used for the study are 0.025 ohm and 1.4 mH which works well for the 2LG faults. These values are obtained based on the grid side filter values of the LCL filter of the GFM inverter. When the fault happens, the grid side voltage drops first, and then the capacitor voltage of the GFM inverter. The VI control essentially takes into account the voltage drop across the filter at the grid side and compensates it in the voltage reference. Instead of using the nominal voltage as voltage reference, this compensated voltage reference respects the constraints of the circuit and therefore the voltage controller is able to achieve this target voltage reference. Note that R and X values are not completely equal to the grid side filter resistance and reactance, but close to them considering there might be errors in measurements of the output current.

The adaptive virtual impedance is designed based on these values. Rearranging the equation (1), we have $V_{od}^{+*} = V_{od}^{+*} + Xi_{oq}^{+} - Ri_{od}^{+}$. Based on the sign of positive components of current (i_{od}^{+} and i_{oq}^{+}), the change direction of R and X can be determined. In this design, the adaptive VI control is triggered only if the absolute value of the steady state tracking error ($e = V_{od}^{+*} - V_{od}^{+}$) is larger than the pre-defined threshold (5 V). Table 2 lists the changes for the R and X for adaptive control. Note that 0.8 and 0.2 are the weighting factors for changing R and X. The adaptive VI control needs to include the logics of detecting steady state of tracking error, and signs of positive current *dq* components.

Table 2 Changes of R and X for adaptive VI control.

Tracking error	V_{od}^{+*}	R	X
$> 5\,V$	Be reduced.	If i_{od}^{+} is positive, incease R by $\frac{0.8e}{i_{od}^{+}}$, otherwise reduce R by $\frac{0.8e}{i_{od}^{+}}$.	If i_{oq}^{+} is postive, reduce X by $\frac{0.2e}{i_{oq}^{+}}$, otherwise increase X by $\frac{0.2e}{i_{oq}^{+}}$.
$< -5\,V$	Be increased.	If i_{od}^{+} is positive, reduce R by $\frac{0.8e}{i_{od}^{+}}$, otherwise increase R by $\frac{0.8e}{i_{od}^{+}}$.	If i_{oq}^{+} is postive, increase X by $\frac{0.2e}{i_{oq}^{+}}$, otherwise reduce X by $\frac{0.2e}{i_{oq}^{+}}$.

V. Simulation Results

In this section, a numerical simulation is performed in MATLAB/Simulink to validate the control performance of the improved control strategy of the GFM inverter in microgrid applications. Simulation of a microgrid with one GFM inverter is performed under asymmetrical and symmetrical faults in islanded mode, and the 1547-2018 compliance testing in grid-connected mode is also tested and validated. The microgrid under study has one GFM inverter, one GFL inverter, and two commercial loads. Note that an average switch model is used to simulate the GFM and GFL inverters because it better represents the inverter behaviors and dynamics than the average model.

A. *Islanded Microgrid with 2LG Fault with 50 ohm Fault Impedance*

Continuing the test shown in Section III, the same fault scenario (2LG fault with 50 Ω fault impedance) is applied at the same time and duration (the fault is applied at 5 s and removed at 7.5 s). The GFL inverter is IEEE 1547-2018 compliant; it disconnects after 2 s (voltage lower than 0.5 p.u.) and reconnects when the terminal voltage is normal. Fig. 5 shows the simulation results of the negative-sequence control only, and Fig. 6 shows the results of the negative-sequence control with VI control.

As shown in Figure 5 (a), the actual positive-sequence *d* component of the GFM inverter voltage has a large discrepancy from its target value (nominal voltage) due to the fault, and the *q* component has small oscillations rather than a straight DC component. As for the negative sequence *dq* component, the *q* component shows discrepancy from its target value (zero). Due to the large tracking error in the positive-sequence *d* component, the PI control in the outer voltage loop will saturate, resulting in the saturated current reference and inner current loop, which cause instability in the output voltage, as shown in Fig. 5 (c). The pulse-width modulation (PWM) signals in Fig. 5 (d) show that the positive-sequence component is saturated with a PWM greater than "1," the negative-sequence PWM is totally distorted and unstable (the period with zero PWM after the fault means that the unbalanced ratio is less than the target level for selecting the negative-sequence control), and the final PWM signal is saturated and distorted. This further explains why the output voltage is distorted and unstable.

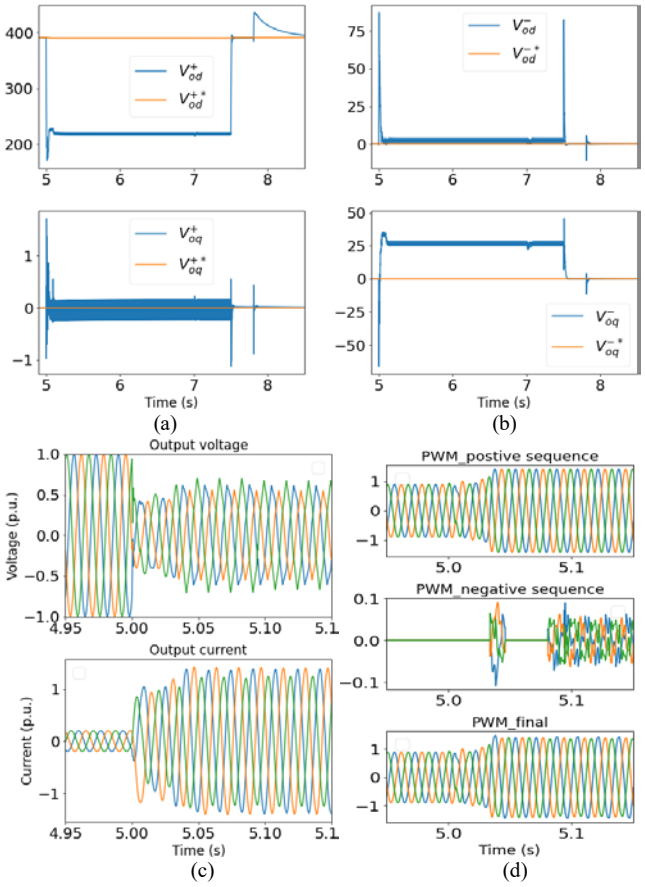

Fig. 5. Simulation results of a GFM inverter with negative-sequence control: (a) the *dq* components of voltage in positive-sequence control; (b) the *dq* components of voltage in negative-sequence control; (c) the output voltage and current of a GFM inverter; and (d) the PWM signals of the inverter: positive sequence (top), negative sequence (middle), and the final signal (bottom).

With the VI control, the GFM inverter improves the stability, as shown in Fig. 6. First, Fig. 6 (a) shows that the positive-sequence *d* component of the GFM inverter voltage tracks its modified reference, which avoids the saturation of the PI control in the voltage loop and the current reference. The *q* component also shows good tracking performance without the oscillations observed in Figure 5 (a). For the negative-sequence control, both the *d* and *q* components track the references well. Figure 6 (a) and (b) indicate that the positive- and negative-sequence control functions behave as expected. Figure 6 (c) shows that the output voltage experiences some transients after fault but quickly reaches steady state with totally compensated and balanced three-phase voltages. The output current is still unbalanced, but the magnitude is smaller than the one observed in Figure 5 (c). The PWM signals in Figure 6 (d) show no saturation in the positive-sequence PWM, stable PWM in the negative-sequence PWM, and an unbalanced final PWM signal for the unbalanced compensation; thus, the PWM signals further validate the stability of the GFM inverter with VI control. Figure 6 demonstrates the effectiveness of the developed negative-sequence control with the VI strategy, and it also indicates the necessity of adding VI control to improve the stability of the GFM inverter for FRT capabilities.

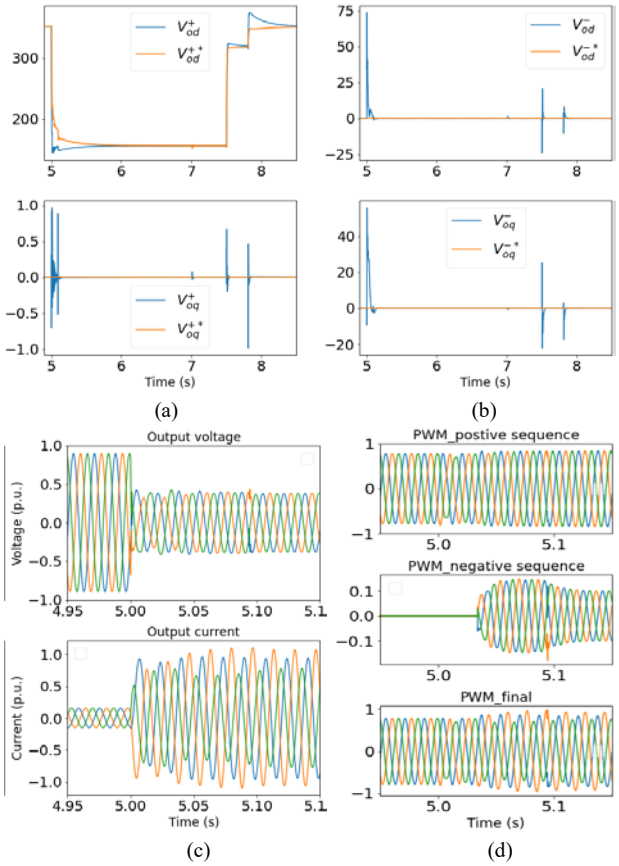

Fig. 6. Simulation results of a GFM inverter with negative-sequence and VI control: (a) the *dq* components of voltage in positive-sequence control; (b) the *dq* components of voltage in negative-sequence control; (c) the output voltage and current of a GFM inverter; and (d) the PWM signals of the inverter: positive sequence (top), negative sequence (middle), and the final signal (bottom).

B. Islanded Microgrid with LG Fault with 0.1 ohm Fault Impedance

To test the adaptive VI control, a LG fault with 0.1 ohm fault impedance is applied at 5 s and removed at 7.5 s. This is a severe fault which causes even larger voltage drop in the GFM inverter capacitance voltage. The designed adaptive VI control in Section IV Part C is applied in this test. The testing results are presented in Fig. 7. Similarly, the GFL inverter disconnects after 2 s (voltage lower than 0.5 p.u.) and reconnects when the terminal voltage is normal. This explains the transients appeared in the voltage components shown in

Fig 7 (a). As seen from Fig. 7 (a), the *d* component of voltage positive sequence reaches steady state with large tracking error (approximately 10 V ≥ 5 V (the threshold)), and then the adaptive virtual impedance is triggered at 6 s to reduce the voltage reference, thus the output voltage (V_{od}^{+}) can reach and track its reference (V_{od}^{+*}). For the virtual impedance, R changes from 0.025 ohm to 0.095 ohm, and L changes from 1.4 mH to 1.45 mH. They keep the same for the rest of simulation time since the tracking error is small and within the threshold. As for the other voltage components shown in Fig 7 (a) and (b), they are designed to track zero voltage reference, and the results show that they track their own references well.

Fig. 7 (c) shows that the GFM inverter generates balanced three phase voltage using the VI control, and the output current of the GFN inverter is unbalanced as designed. For the PWM signals, the positive and negative sequence both experience transients after fault and reach steady state with balanced waveforms, thus resulting the final PWM reach steady state with unbalanced waveforms to compensate the negative sequence voltage. The results presented in Fig. 7 validate the effectiveness of the designed adaptive VI control to improve the tracking performance of voltage control, and further improve the stability of the GFM inverter.

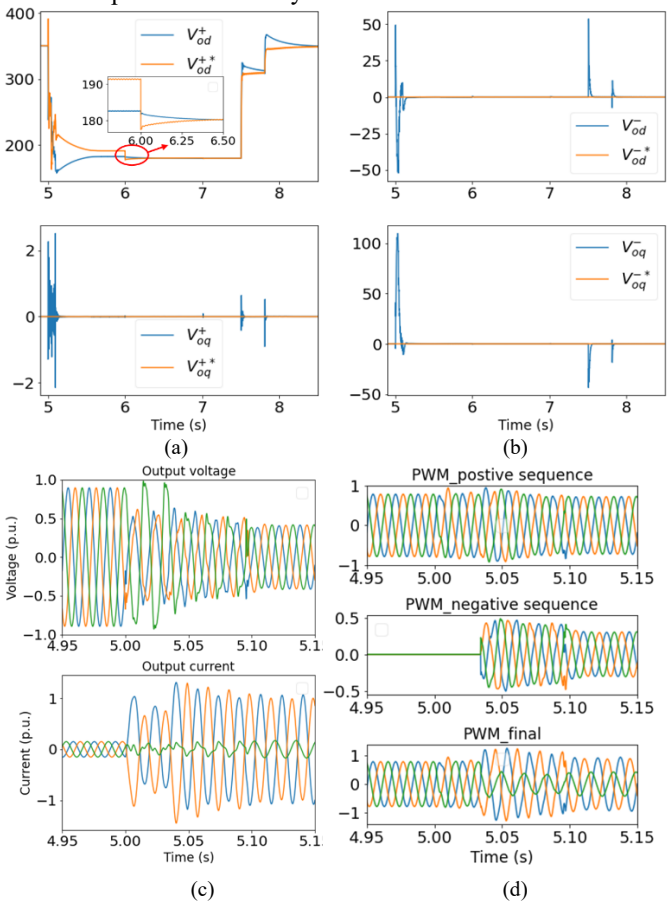

Fig. 7. Simulation results of a GFM inverter with negative-sequence and adaptive VI control: (a) the *dq* components of voltage in positive-sequence control; (b) the *dq* components of voltage in negative-sequence control; (c) the output voltage and current of a GFM inverter; and (d) the PWM signals of the inverter: positive sequence (top), negative sequence (middle), and the final signal (bottom).

C. *Islanded Microgrid with High and Low Impedance Faults*

To further evaluate the performance of the improved control structure of the GFM inverter for FRT capabilities, more tests are performed for the islanded microgrid with high and low impedance faults. The balanced faults (e.g., 3LG) are also studied to test the adaptive VI control, and the negative sequence control is not activated due to the balanced output current in the GFM inverter. Overall, the proposed improved control structure for FRT capabilities works well for all the high and low impedance faults tested, most faults studied can achieve good tracking performance without changing the virtual impedance, and the inverter output voltage is balanced after compensation. The test results of adaptive VI control with the final impedance values are summarized in Table 3.

Table 3 Summary of various fault testing.

Fault	Virtual impedance
LG, 0.1 ohm	R_VI=0.065; L_VI=1.4e-3
LG, 100 ohms	R_VI=0.065; L_VI=1.4e-3
LLG, 0.1 ohm	R_VI=0.025; L_VI=1.43e-3
LLG, 50 ohms	R_VI=0.025; L_VI=1.4e-3
LL, 0.1 ohm	R_VI=0.025; L_VI=1.4e-3
LL, 100 ohms	R_VI=0.025; L_VI=1.4e-3
3LG, 1 ohm	R_VI=0.025; L_VI=1.4e-3
3LG, 100 ohms	R_VI=0.0138; L_VI=0.77e-3

D. *Grid-Connected Microgrid with LG Fault with 0.1 ohm Fault Impedance*

This scenario is to test the GFM inverter's DER response to abnormal voltages during grid-connected mode for 1547-2018 compliant test. A LG fault with 0.1-ohm fault impedance is applied to the bus where the GFM inverter is connected from 6 s to 8.5 s. With this low impedance, the inverter PCC voltage drops below 0.5 p.u. Based on the IEEE 1547-2018, the inverter should enter momentary cessation mode that the DER generates pre-fault power for the first 5 cycles and zero power thereafter until trip (if the voltage stays lower than 0.5 p.u. for 2 s, the inverter should trip). Since the fault is removed at 8.5 s, the inverter should trip at 8 s. The representative results are presented in Fig. 8 and Fig. 9.

Fig. 8 (a) and (b) shows the measured active and reactive power of the GFM inverter in grid-connected mode. Before the fault happens, the GFM inverter can track the power references; when the fault happens, the inverter keeps the pre-fault power for five cycles, then generates zero power afterwards until trips at 8 s; and the inverter is reconnected to the main grid at 10 s and continues to generate the commanded power. Fig. 8 (c) and (d) shows the phase A output voltage and current of the GFM inverter. Since the fault is removed at 8.5 s, the inverter is programmed to resynchronize with the main grid once the PCC voltage is back to normal. Note that during the momentary cessation (between 6 s and 8 s), the GFM inverter still generates voltage output because it stays standby in case the system voltage is back to normal.

Fig. 9 shows the logic signals related to the implementation. The "Block_signal" is applied in the voltage and current controllers to zero out the voltage and current references, and the "Trip_signal" is applied at the circuit breaker control logic to trip off the GFM inverter after the threshold time. The results show that the logic signals work as expected, which results in the inverter follow the DER response as defined in IEEE 1547-2018.

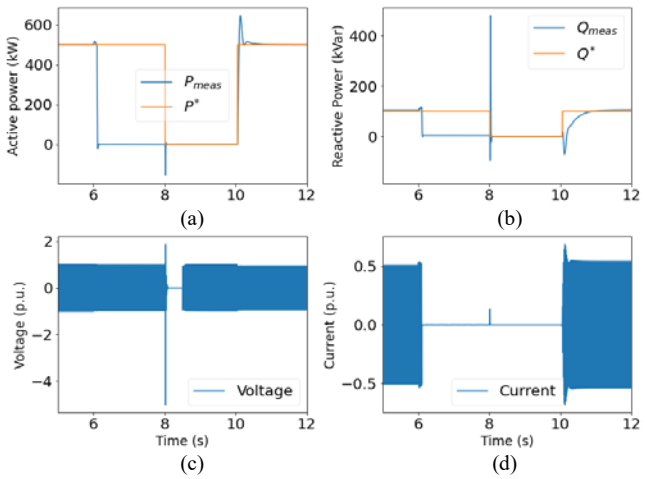

Fig. 8. Simulation results of a GFM inverter in grid-connected mode (a) the active power reference and output; (b) the reactive power reference and output; (c) phase A of output voltage; and (d) phase A of output current.

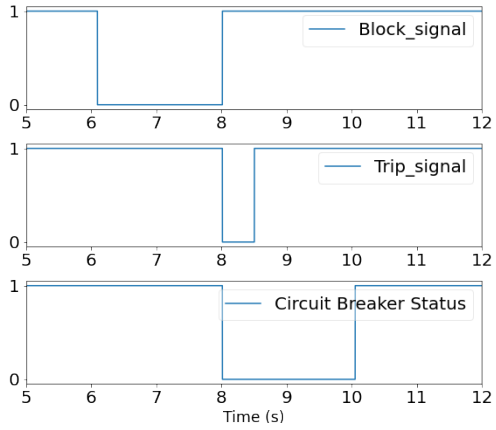

Fig. 9. Logic signals of the GFM inverter: block signal (top), trip signal (middle) and the circuit breaker status (bottom).

VI. Conclusion

This paper presents an improved control strategy of GFM inverters for FRT capabilities to achieve balanced three-phase voltages under asymmetrical faults—starting from the equivalent circuits of the three types of asymmetrical faults, then investigating the inverter behaviors under a 2LG fault, and finding that the inverter might become unstable under more severe faults. Next, the negative-sequence control is proposed together with the VI strategy. Unlike existing works, only the *d* component of the positive-sequence control is proposed and proven needing the VI control. The negative-sequence control only and the negative-sequence control with the VI strategy are simulated with the 2LG fault. The results show that the inverter using only the negative-sequence control is unstable because the fault causes a large voltage drop in the inverter, thus causing a large tracking error in the voltage loop and saturated current references and an inner current loop. With the VI control reducing the voltage reference, the voltage *d* component can track the reachable reference, and there is no tracking error in the voltage loop and saturation of the current reference, thus improving the stability of the GFM inverter and achieving the target balanced voltages. Moreover, the adaptive tuning of the VI control is proposed due to the necessity of making the VI control work in all fault conditions, and simulation results have demonstrated the efficacy of the proposed adaptive VI control. Lastly, the voltage response of GFM inverter is studied under grid-connected mode, indicating the expected response to abnormal voltage causes by fault.

Acknowledgment

This work was authored by the National Renewable Energy Laboratory, operated by Alliance for Sustainable Energy, LLC, for the U.S. Department of Energy (DOE) under Contract No. DE-AC36-08GO28308. This work was supported by the Laboratory Directed Research and Development (LDRD) Program at NREL. The views expressed in the article do not necessarily represent the views of the DOE or the U.S. Government. The U.S. Government retains and the publisher, by accepting the article for publication, acknowledges that the U.S. Government retains a nonexclusive, paid-up, irrevocable, worldwide license to publish or reproduce the published form of this work, or allow others to do so, for U.S. Government purposes.

References

[1] R. Lasseter, Z. Chen, and D. Pattabiranman, "Grid-Forming Inverters: A Critical Asset for the Power Grid," *IEEE Journal of Emerging and Selected Topics in Power Electronics*, vol. 8, no. 3, June 2020, pp. 925-935.

[2] P. Piya, M. Ebrahimi, M. Ghartemani, and S. Khajehoddin, "Fault-Ride-Through Capability of Voltage-Controlled Inverter," *IEEE Trans. On Ind. Electr.*, vol. 65, no. 10, Oct. 2018.

[3] N. Bottrell and T. C. Green, "Comparison of Current-Limiting Strategies during Fault Ride-Through of Inverters to Prevent latch-up and Wind-up," *IEEE Tran. on Power Electr.*, vol. 29, no. 7, July 2014, pp. 3786-3797.

[4] Z. Shuai, et al., "Charactersitics and Restriain Method of Fast Transient Inrush Fault Currents in Synchron-verters," IEEE Tran. on Ind. Electr., vol. 64, no. 9, Sep. 2017.

[5] S. F. Zarei, et al., "Reinforcing Fault Ride Through Capability of Grid Forming Voltage Source Converters Using an Enhanced Voltage Control Scheme," *IEEE Tran. on Power Del.*, vol. 34, no. 5, Oct. 2019, pp. 1827-1842.

[6] B. Mahamedi, M. Eskandari, J. Fletcher, J. Zhu, "Sequence-Based Control Strategy with Current Limiting for the Fault Ride-Through of Inverter-Interfaced Distributed Generators," *IEEE Tran. on Sus. Energy*, vol. 11, no. 1, Jan. 2020, pp. 165-174.

[7] R. Rosso, S. Engelken, M. Liserre, "Current Limitation Strategy For Grid-Forming Converters Under Symmetrical and Asymmetrical Faults," *2020 IEEE Energy Conversion Congress and Exposition (ECCE)*, 11-15 Oct. 2020, Detroit, MI, USA.

[8] Jing Wang, "Design Power Control Strategies of Grid-Forming Inverters for Microgrid Application," *2021 IEEE Energy Conversion Congress and Exposition (ECCE)*, 10-14 Oct. 2021, Vancouver, BC, Canada.

[9] N. Gurule, et al., "Experimental Evaluation of Grid-Forming Inverters Under Unbalanced and Fault Conditions," *2020 The 46th Annual Conference of the IEEE Indutrial Electornics Society*, 18-21 Oct. 2020, Singapore.

[10] R. Teodorescu, M. Liserre, and P. Rodriguez, *Grid Converters for Photovoltaic and Wind Power Systems*, NJ, USA: Wiley-IEEE Press, 2011.